INL/CON-07-13222
PREPRINT

Application of Gamma Code Coupled with Turbomachinery Models for High Temperature Gas-Cooled Reactors

ISROMAC 12

C. H. Oh
E. S. Kim
S. Sherman
J. H. Kim
H. C. No

February 2008

The 12th International Symposium on Transport Phenomena and Dynamics of Rotating Machinery
Honolulu, Hawaii, February 17-22, 2008

ISROMAC12-2008-20224*

APPLICATION OF GAMMA CODE COUPLED WITH TURBOMACHINERY MODELS FOR HIGH TEMPERATURE GAS-COOLED REACTORS

C.H. Oh, E.S. Kim, S. Sherman, J.H. Kim, and H.C. NO

Idaho National Laboratory, P.O. Box 1625, Idaho Falls, ID.83415 and KAIST, Daejeon, Korea.
208-526-7716/208-526-0528 and 82-42-869-3817
Chang.Oh@inl.gov, Eungsoo.Kim@inl.gov, steven.sherman@inl.gov,
jhkim@kaist.ac.kr,hcno@kaist.ac.kr

ABSTRACT

The very high-temperature gas-cooled reactor (VHTR) is envisioned as a single- or dual-purpose reactor for electricity and hydrogen generation. The concept has average coolant temperatures above 900^{0}C and operational fuel temperatures above 1250^{0}C. The concept provides the potential for increased energy conversion efficiency and for high-temperature process heat application in addition to power generation. While all the High Temperature Gas Cooled Reactor (HTGR) concepts have sufficiently high temperature to support process heat applications, such as coal gasification, desalination or cogenerative processes, the VHTR's higher temperatures allow broader applications, including thermochemical hydrogen production. However, the very high temperatures of this reactor concept can be detrimental to safety if a loss-of-coolant accident (LOCA) occurs. Following the loss of coolant through the break and coolant depressurization, air will enter the core through the break by molecular diffusion and ultimately by natural convection, leading to oxidation of the in-core graphite structure and fuel. The oxidation will accelerate heatup of the reactor core and the release of a toxic gas, CO, and fission products. Thus, without any effective countermeasures, a pipe break may lead to significant fuel damage and fission product release. Prior to the start of this Korean/United States collaboration, no computer codes were available that had been sufficiently developed and validated to reliably simulate a LOCA in the VHTR. Therefore, we have worked for the past three years on developing and validating advanced computational methods for simulating LOCAs in a VHTR.

GAMMA code is being developed to implement turbomachinery models in the power conversion unit (PCU) and ultimately models associated with the hydrogen plant. Some preliminary results will be described in this paper.

INTRODUCTION

The VHTR reference concepts are helium-cooled, graphite-moderated, thermal neutron spectrum reactors with an outlet temperature while initially set up to 1000^{0}C. The high temperature will allow the reactor to be used for a large number of process heat applications, including hydrogen production.

The VHTR reactor core could be either a prismatic graphite block type core or a pebble bed core. Use of various working coolants is also being evaluated (Oh et al., 2006). The process heat for hydrogen production will be transferred to the hydrogen plant through an intermediate heat exchanger (IHX). The reactor thermal power and core configuration will be designed to assure passive decay heat removal without fuel damage during hypothetical accidents. The fuel cycle will be a once-through very high burnup low-enriched uranium fuel cycle.

The basic technology for the VHTR (Macdonald et al., 2004) has been established in the former high-temperature gas-cooled reactor test and demonstration plants (DRAGON, Peach Bottom, AVR, Fort St. Vrain, and THTR). In addition, the technologies for the VHTR are being advanced in the Gas Turbine-Modular Helium Reactor (GT-MHR) Project (General Atomics, 1996), and the South African state utility ESKOM sponsored project to develop the Pebble Bed Modular Reactor (PBMR) (Nicholls, 2000). Furthermore, the Japanese HTTR and Chinese HTR-10 test reactors are demonstrating the feasibility of some of the planned VHTR components and materials. (The HTTR is expected to reach a maximum coolant outlet temperature of 950^{0}C in 2003 or 2004.) Therefore, the VHTR project is focused on building a demonstration reactor, rather than simply confirming the basic feasibility of the concept.

One or more technologies will use heat from the high-temperature helium coolant to produce hydrogen. The first technology of interest is the thermochemical splitting of water into hydrogen and oxygen. There are a large number of thermochemical processes that can produce hydrogen from water, the most promising of which are sulfur-based and include the sulfur-iodine, hybrid sulfur-electrolysis, and sulfur-bromine processes (which operate in the 750 to 1000 C range). The second technology of interest is thermally assisted electrolysis of water. The high-efficiency Brayton cycle enabled by the VHTR may be used to generate the hydrogen from water by electrolysis. The efficiency of this process can be substantially improved by heating the water to high-temperature steam before applying electrolysis.

NOMENCLATURE

a_q	acceleration of a fluid particle in the *q* direction [m/s²]
a_{sf}	specific solid-to-fluid interfacial area (m^{-1})
C	concentration
D_{sk}	multi-component diffusion coefficient (m^2/s)
$\mathbf{D}_{sk}$	binary diffusion coefficient (m^2/s)
F_{ij}	geometric view factor
$\mathbf{g}$	gravitational constant (m/s^2)
h_{sf}	interfacial heat transfer coefficient (W/m^2-K)
Δh_f^o	latent heat of formation for chemical reaction (J/kg)
H	sensible enthalpy of gas mixture (J/kg)
h_0	stagnation enthalpy [J/kg-K]
H_s	sensible enthalpy of species, s (J/kg)
J_i	radiosity of the radiating surface, i (W/m^2)
$\mathbf{J}_s$	total diffusion flux with respect to mass average velocity (kg/m^2-s)
K	permeability
m	total number of species (Eq. 3 to 9)
m	meridional direction (Eq. 10 to 12)
P	total pressure (Pa)
q	quasi-orthogonal distance [m]
q'''	volumetric heat source at the wall (W/m^3)
q_r''	net radiative heat flux (W/m^2)
r	radius from rotating axis [m]
r_c	radius of streamline curvature [m]
$\overline{R}$	universal gas constant
R_s	generation/dissipation of species, s, by chemical reaction (kg/m^3-s)
s	pitch length [m], entropy [J/kg]
T_f	temperature of gas mixture (K)
$\overline{T}_k$	temperature of agglomerated surface, k (K)
T_p	solid or pebble temperature (K)
$\mathbf{u}$	mass average velocity of gas mixture (m/s)
V	absolute velocity [m/s²]
W	molar weight of gas mixture (g/mol)
W_s	molar weight of species, s (g/mol)
X_s	mole fraction of species, s
Y_s	mass fraction of species, s, in the bulk, and Y_s^w at the surface of the wall

Greek

α	absolute angle [º], angle between *q* and *m* [º]
ε_k	emissivity of surface k
φ	porosity
ρ	density of gas mixture (kg/m^3)
$(\rho C)_p$	volumetric heat capacity of solid (or pebble) (J/m^3-K)
λ_f	thermal conductivity of gas mixture (W/m-K)
λ_{eff}	effective thermal conductivity in a pebble bed (W/m-K)
λ_{disp}	thermal conductivity induced by thermal dispersion (W/m-K)
μ	viscosity of gas mixture (kg/m-s)

Subscripts

f	fluid
p	pebble

GAMMA CODE

GAMMA code was developed specifically for air ingress analysis for VHTR as part of ROK/US I-NERI project (Oh et al., 2006). The governing equations and numerical methods adopted for this project are described below.

The multi-dimensional governing equations for a chemically reacting flow (Poinsot and Veyannts, 2001) consist of the basic equations for continuity, momentum conservation, energy conservation of the gas mixture, and the mass conservation of each species. Six gas species (He, N_2, O_2, CO, CO_2, and H_2O, (NO, 2004)) are considered in the present analytical model, and it is assumed that each gas species and the gas mixture follow the equation of state for an ideal gas. The GAMMA code has the capability to handle the thermo-fluid and chemical reaction behaviors in a multi-component mixture system as well as heat transfer within the solid components, free and forced convection between a solid and a fluid, and radiative heat transfer between the solid surfaces. Also, the basic equations are formulated with a porous media model (Nield and Bejan, 1999) to consider heat transport in a pebble-bed core) as well as solid-fluid mixed components.

The equation of continuity for the gas mixture:

$$\varphi \frac{\partial \rho}{\partial t} + \nabla \cdot (\rho \mathbf{u}) = \varphi \sum_s R_s \qquad (1)$$

The equation of momentum conservation:

$$\rho\left(\frac{1}{\varphi}\frac{\partial \mathbf{u}}{\partial t} + \frac{1}{\varphi^2}\mathbf{u}\cdot\nabla\mathbf{u}\right) = -\nabla P + \frac{1}{\varphi}\nabla\cdot(\mu\nabla\mathbf{u}) - \frac{\mu}{K}\mathbf{u} - \frac{C_F\rho}{\sqrt{K}}|\mathbf{u}|\mathbf{u} + \rho\mathbf{g} \qquad 2)$$

The equation of sensible energy conservation:

$$\varphi\frac{\partial}{\partial t}(\rho H) + \nabla\cdot(\rho\mathbf{u}H) = \nabla\cdot\left[\left(\varphi\lambda_f + \lambda_{disp}\right)\nabla T_f\right] - \nabla\cdot\left(\varphi\sum_{s=1}^{m} H_s\mathbf{J}_s\right) - \varphi\sum_s \Delta h^o_{f_s} R_s + h_{sf}a_{sf}\left(T_p - T_f\right) \qquad (3)$$

The conservation equation of each species, s:

$$\varphi\frac{\partial}{\partial t}(\rho Y_s) + \nabla\cdot(\rho\mathbf{u}Y_s) = -\nabla\cdot(\varphi\mathbf{J}_s) + \varphi R_s \qquad (4)$$

and for He, $Y_m = 1 - \sum_{s=1}^{m-1} Y_s$

The equation of state for an ideal gas:

$$\rho = \frac{P}{\bar{R}T}\left(\sum_{s=1}^{m} Y_s / W_s\right)^{-1} \qquad (5)$$

For a solid and a pebble bed, the same heat conduction equation is used. A thermal non-equilibrium model for porous media is used to consider the heat exchange between the fluid and the pebbles as follows:

$$\left[(1-\varphi)(\rho C)_p\right]\frac{\partial T_p}{\partial t} = \nabla\cdot\left(\lambda_{eff}\nabla T_p\right) + q''' - h_{sf}a_{sf}\left(T_p - T_f\right) \quad (6)$$

Radiative heat transfer in the enclosure is well-modeled by using an irradiation/radiosity method (Holman, 1986) which assumes that the fluid is non-participating and the radiation exchange between surfaces is gray and diffuse. The net radiative flux from agglomerated surface k, which consists of N_k faces of the original mesh, is given by

$$q''_{rk} = \left[\left(\sum_{j\neq k}^{M} F_{kj}\right)\varepsilon_k \bar{T}_k^{\,4} - \varepsilon_k \sum_{j\neq k}^{M} F_{kj} J_j\right]\left[\varepsilon_k + (1-\varepsilon_k)\sum_{j\neq k}^{M} F_{kj}\right]^{-1}$$

$$J_j = \varepsilon_j C_j \sigma \bar{T}_j^{\,4} + (1-\varepsilon_j) C_j \sum_{i\neq j}^{M} F_{ji} J_i \qquad (7)$$

The ordinary diffusion flux (J_s) is given in two forms, the full multi-component diffusion (Hirschfelder et al., 1964) and the effective diffusion (Kays and Crawford, 1980) by the assumption that a dilute species, s, diffuses through a homogeneous mixture:

$$\mathbf{J}_s = \rho\frac{W_s}{W^2}\sum_{k=1,k\neq s}^{m}\left[D_{sk}\nabla\left(Y_k W\right)\right] \qquad (8)$$

$$\mathbf{J}_s = -\rho D_{s-mix}\nabla Y_s \quad where \quad D_{s-mix} = \left(\sum_{k=1,k\neq s}^{m} X_k / \mathbf{D}_{sk}\right)^{-1} \quad (m \geq 3) \qquad (9)$$

Although Eq. (8) predicts the accurate diffusion behaviors of species in a multi-component mixture, Eq. (9) is generally used in numerical calculation because of its computational efficiency and its accuracy close to that of Eq. (8). Physical properties, such as molar weight, viscosity, thermal conductivity, and sensible enthalpy, for each gas component and gas mixtures, are obtained from the handbooks of gas properties (Poling et al., 2001 and Raznjevic, 1976).

VERIFICATION OF GAMMA CODE

Gamma code is based on the 1st order differencing accuracy and Gamma code was verified using Fluent code with the 2nd order differencing accuracy. Inverse U-tube (Figure 1) data were used for this comparison calculation.

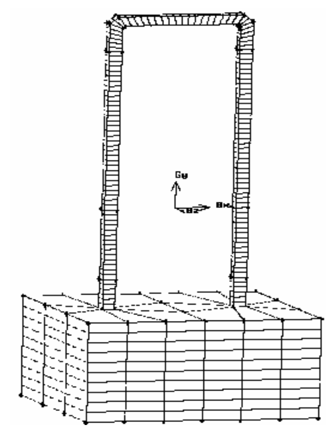

Figure 1. Fluent meshing on inverse U-tube.

Figure 2 shows comparison of test data, results from the Implicit Continuous Eulerian (ICE) technique used in Gamma code using 1st order accuracy , results from Fluent using the second order accuracy.

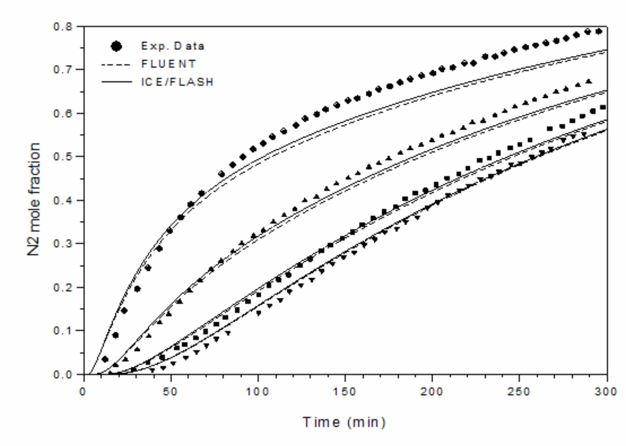

Figure 2. Comparison of results from gamma and Fluent.

Table 1 shows verification and validation of Gamma code using various data (Oh et al., 2006).

* D : Diffusion
* NC : Natural Convection
* R: Radiation
* C: Chemical Reaction
* P: Porous Media

	Test Facility	D	NC	R	C	P	etc
1	Pipe Network						O
2	Blowdown	O					O
3	Buncan & Toor's Experiment	O					
4	Inverse U-tube single/multiple channel test	O	O				
5	Ogawa's circular tube test				O		
6	Takahashi's annular tube test				O		
7	VENTURA pebble bed test				O	O	
8	Inverse U-tube air ingress experiment	O	O		O		
9	HTTR simulated air ingress experiment	O	O		O		O
10	Vertical slot experiment	O	O				
11	NACOK natural convection test		O			O	
12	SANA-1 afterheat removal test					O	
13	SNU RCCS test		O	O			

TURBO MACHINERY MODEL

We envision GAMMA code to be an integrated computer code for analyzing the HTGR coupled with hydrogen production plant . This means that we need to include the turbomachinery model and hydrogen production related model to GAMMA in the near future. Actually as part of this task, turbomachinery models are being developed (Kim et al., 2006) and are being linked to GAMMA code. The methodology of the model and some results are presented in this section.

The flow in multi-stage gas turbine is inherently three-dimensional. It is necessary to simplify the flow as having an intermediate level of sophistication, because the real flow process in a multistage gas turbine is exceedingly complex. The flow is assumed to be inviscid and may be regarded as being obtained by circumferentially averaging all flow properties, and then the loss effects are added on to the throughflow solution.

From the assumption of axisymmetric and inviscid flow it is possible to define a series of meridional stream surfaces and there are surfaces of revolution along which fluid particles are assumed to move through the gas turbine. In typical multi-stage axial compressor or turbine, the streamlines change radius along the axial length of the component, and the calculation of the flow along the hub to tip surface is usually referred to as the throughflow method (Cumpsty, 1989).

In the view of the meridional plane, Figure 3, the typical quasi-orthogonal lines and stream surface are illustrated. According to the description and approach given by Denton (1978), the acceleration of a fluid particle at P can be built up from the following components: $V_m \partial V_m / \partial m$ in the m direction, $-V_\theta^{\,2}/r$ in the radial direction, and $V_m^{\,2}/r_c$ in the normal to the m direction. With the blade loading to be neglected, these three acceleration components can be combined to give the total acceleration a_q in the direction of the quasi-orthogonal line

$$a_q = V_m \frac{\partial V_m}{\partial m}\cos\alpha + \frac{V_m^{\,2}}{r_c}\sin\alpha - \frac{V_\theta^{\,2}}{r}\sin(\phi+\alpha) \qquad (10)$$

The momentum equation and energy equation applied in the stream surface is then

$$\frac{1}{2}\frac{d}{dq}V_m^{\,2} = \frac{dh_0}{dq} - T\frac{ds}{dq} - \frac{1}{2r^2}\frac{d\left(r^2 V_\theta^2\right)}{dq} + \frac{V_m^2}{r_c}\sin\alpha + V_m\frac{dV_m}{dm}\cos\alpha \qquad (11)$$

and the total mass flow rate across the quasi-orthogonal is given by`

$$\dot{m} = \int_A^B 2\pi r \rho V_m \sin\alpha \; dq \qquad (12)$$

so that the meridional velocity and streamline curvature can be calculated from these two equations.

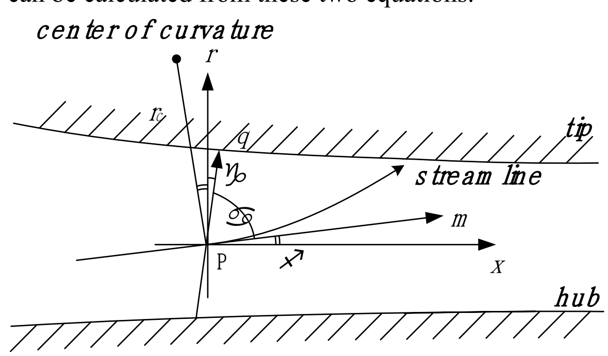

Figure 3.Quasi-orthogonal line in the meridional plane

The GTHTR 300 compressor design of JAEA (Takizuka et al., 2004) has been selected to verify the code results. This particular unit has been chosen because the details of the compressor geometry and overall performance are available. Table 1 shows a summary of the design parameters. This compressor has a high reaction stage design and a constant inner wall diameter with high hub-tip ratio throughout 20 stages. In table 2, the predictions by the present code are compared with the design-point performance of JAEA data. This table shows that the pressure and temperature conditions are well satisfied with the design-point loss estimation. The fluid properties and velocities in the compressor are calculated and the representative examples are shown in Figure 8 and 9. By modifying the loss models, this code is capable of estimating the performance of a wide range operation. The predicted pressure ratio results are compared with the reference data in Figure 10. The pressure ratio variation with the change of mass flow shows excellent agreement and the surge margin is also well predicted. While the reference shows 30% of surge margin, the code result is 30.9%. The JAEA data were replotted on the non-dimensional basis, polytropic efficiency against the corrected mass flow rate in Figure 11. The code result shows good agreement compared with the reference and the general trends of variation are well observed. The efficiency was slightly overestimated at low rotational speed with a RMS error about 3 percent.

Table 1. Specifications of GTHTR 300 Compressor.

Mass flow rate (kg/s)	449.7
Inlet temperature (°C)	28
Inlet pressure (MPa)	3.52
Pressure ratio	2.0
Hub diameter (mm)	1500
Tip diameter (1st/20th stage, mm)	1704/1645
Number of stages	20
Rotational speed (rpm)	3600
Number of rotor/stator blades (1st stage)	72/94
Polytropic efficiency (%)	90.5

Table 2. Comparison of design-point performance.

Parameters	JAEA	KAIST	Error (%)
Pressure ratio	2.00	1.98	-1.00
Temperature ratio	1.36	1.35	-0.66
Polytropic efficiency(%)	90.5	90.7	0.22
Shaft Work (MW)	251	246	-1.99

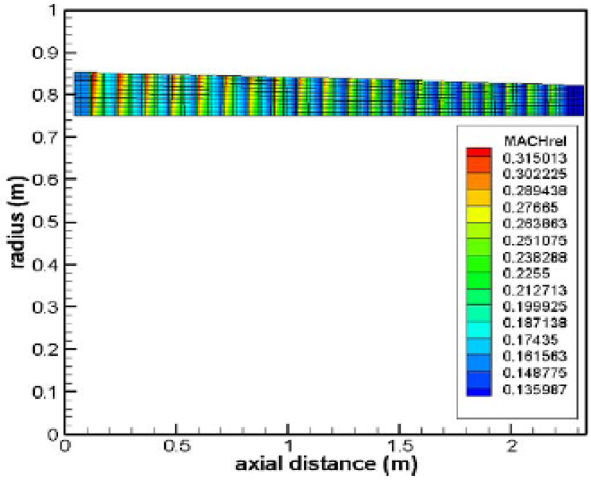

Figure 4. Relative Mach number in the compressor.

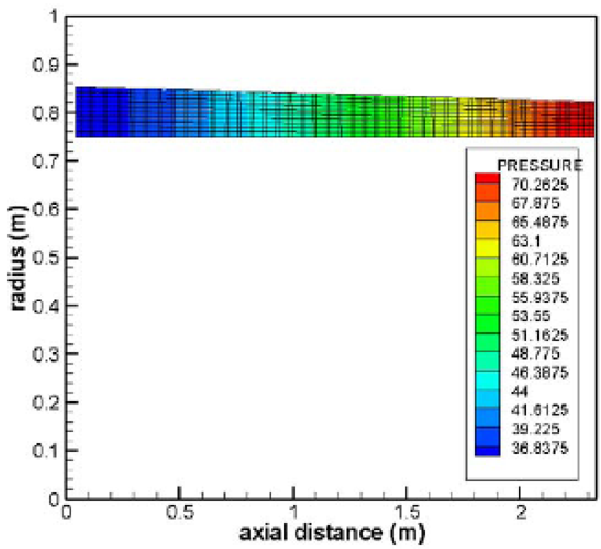

Figure 5. Total pressure in the compressor.

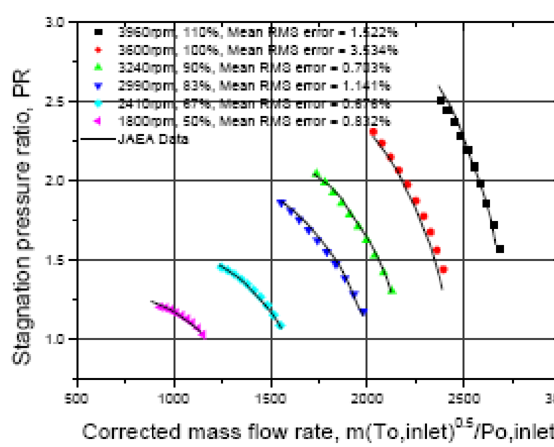

Figure 6. Pressure ratio vs. mass flow characteristics of GTHTR 300 compressor.

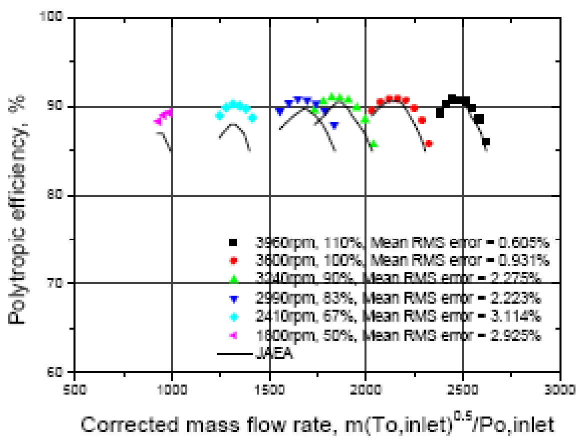

Figure 7. Efficiency vs. Mass flow characteristics of GTHTR 300 compressor.

COUPLING OF VHTR AND HTSE

In this study, the following five different configurations of the integrated system are evaluated in terms of the overall hydrogen production efficiency and only once configuration is presented in this paper. Configurations studied are as follows.

(1) Configuration 1 - Indirect Parallel Cycle (Figures 8 and 9)

(2) Configuration 2 - Indirect Serial Cycle (Oh et al., 2007)

(3) Configuration 3 - Direct Serial Cycle (Oh et al., 2007)

(4) Configuration 4 - Steam Combined Cycle (Oh et al., 2007)

(5) Configuration 5 - Reheat Cycle (Oh et al., 2007)

Figure 8 illustrates the indirect parallel system. The flow in the secondary coolant system is divided, with most of the flow going towards the PCU and the remainder going through a secondary heat exchanger (SHX) that directs heat towards the HTSE plant. The flow through the hot side of the SHX is then mixed with the flow from the PCU to feed the cold side of the intermediate heat exchanger (IHX). However, some of the flow is diverted away from the PCU, which acts to decrease the efficiency of the cycle. There are three coolant loops. The primary coolant system contains the nuclear reactor, the hot side of the IHX, and a compressor. The secondary coolant system contains the cold side of the IHX, the hot side of the SHX, the PCU, and connecting piping, which is assumed to be short. The intermediate heat transport loop connects the secondary coolant system to the HTSE plant through several process heat exchangers (PHXs).

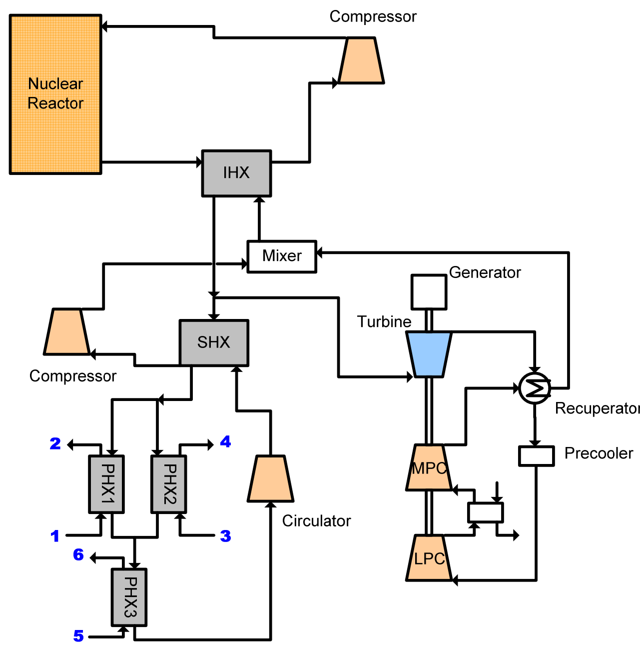

Figure 8. Configuration 1 - indirect parallel cycle.

For electrolysis, the steam is heated up to higher than 800 °C by the heat from SHX. The heated steam is converted into hydrogen and oxygen in the electrolyzer and discharged through the fuel and oxidizer outlet, respectively as shown in Figure 9. The heat of the discharged gases is recovered through three recuperators. Finally, the product gas in the fuel side contains hydrogen and steam, and the oxidizer outlet gas contains oxygen and steam. As shown in Figure 9, the discharged fuel steam is recycled to the inlet fuel stream, and the hydrogen gas is separated and collected in the separator. In the oxidizer outlet stream heat is first recuperated and then the stream is run through an expander to recover work. The oxygen and water components of the stream are then separated.

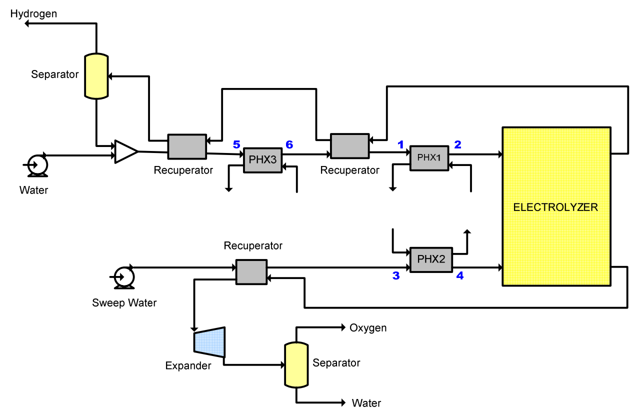

Figure 9. HTSE system.

CONCLUSIONS

GAMMA code that has been developed as part of ROK/US –I-NERI project has been verified using a number of experimental results. Results from GAMMA code agree very well with the inverse U-tube experiments results. Turbomachinery models that were developed separately using the Newton-Ralphson method to improve the convergence and to make more detailed calculations of the turbomachinery were verified well with GTHTR 300 turbomachinery design basis with good agreements. The coupling scheme of VHTR and the high temperature steam electrolysis process to produce hydrogen using the nuclear energy has been proposed. We will implement the turbomachinary models and the hydrogen production model of the high temperature steam electrolysis into GAMMA code in the near future.

REFERENCES

Cumpsty, N.A., “Compressor Aerodynamics”, Longman Scientific & Technical ,1989.

Denton, J.D., “Throughflow Calculation for Transonic Axial Flow Turbines,” Journal of Engineering for Power, Transactions of the ASME, Vol. 100, pp. 212-218 ,1978.

General Atomics, *Gas Turbine-Modular helium Reactor (GT-MHR) Conceptual Design Description Report*, 910720, Revision 1, July, 1996.

Hirschfelder, J.O., , C. F. Curtiss., and R. B. Bird , Molecular Theory of Gases and Liquids, John Wiley & Sons, New York ,1964.

Holman, J. P., 1986, Heat Transfer, Sixth Edition, McGraw-Hill Book Company, New York.

Kayes, W. M. and M.E. Crawford, *Convective Heat and Mass Transfer, Second Edition*, McGraw-Hill Book Company, New York, 1980.

Kim, J. H., H. M. Kim, H. C. NO, Assessment of HTGR Helium Compressor Analysis Tool based on Newton-Ralphosn Numerical Application to Throughflow Analysis, ICONE14-89411, July 17-20, Miami, Florida, 2006.

Macdonald, P.E., et al., “The Next Generation Nuclear Plant- Insights gained from the INEEL Point Design Studies,” INEEL, INEEL/CON-04-01563, 2004.

Nicholls, D.R., “Status of the Pebble Bed Modular Reactor,” *Nuclear Energy* **39**, No.4, 2000.

Nield, D.A. and A. Bejan A., Convection in Porous Media, Springer-Verlag, New York ,1999.

Oh, C.H., C. Davis, L. Siefken, R. Moore, H. C. NO, J. Kim, G. C. Park, J.C. Lee, and W. R. Martin, “Development of Safety Analysis Codes and Experimental Validation for a Very High Temperature Gas-Cooled Reactor,” Final Report, Idaho National Laboratory, INL/EXT-06-01362, March 2006.

Oh, C.H., Kim, E.S., Sherman, S.R., Vilim, R., Lee, Y.J., Lee, W.J., HyPEP FY-07 Annual Report: A Hydrogen production Plant Efficiency Calculation Program, INL/EXT-07-13078, September 2007.

Oh, C.H., R. Barner, C. Davis, and S. Sherman, “Evaluation of Working Fluids in an Indirect Combined Cycle in a Very High Temperature Gas-Cooled Reactor,” *Nuclear Technology* , Vol.156, No.1, 2006.

Poinsot, T. and D. Veynante , Theoretical and Numerical Combustion, R.T. Edwards Inc., 2001.

Poling, B.E., J. M. Prausnitz, and J. P. O'Connell,2001. The Properties of Gases and Liquids, Fifth ed., McGraw-Hill, New York.

Raznjevic, K., 1976. Handbook of Thermodynamic Tables and Charts, Hemisphere, Washington.

Takizuka, T., S. Takata, X. Yan, S. Kosugiyama, S. Kantanishi and K. Kumitomi, “R&D on the Power Conversion System for Gas Turbine High Temperature Reactors,” Nuclear Engineering and Design, North-Holland Publishing Company, pp.329-346, 2004.